SPACE SURVEILLANCE OBSERVATIONS AT THE ZIMMERWALD OBSERVATORY

Martin Ploner[1], Thomas Schildknecht[2], Carolin Früh[3], Alessandro Vananti[4], Johannes Herzog[5]

Astronomical Institute, University of Bern, Sidlerstrasse 5, 3012 Bern, Switzerland
[1]*ploner@aiub.unibe.ch,* [2]*schildkncecht@aiub.unibe.ch,* [3]*frueh@aiub.unibe.ch,* [4]*vananti@aiub.unibe.ch,*
[5]*herzog@aiub.unibe.ch*

ABSTRACT

At the Zimmerwald observatory optical observations of artificial space objects are performed with the 1m Laser and Astrometric Telescope ZIMLAT and the 0.2m Small Robotic Telescope ZimSMART. While ZIMLAT is especially used for follow-up observations of newly detected small-size space debris objects, the main field of application of ZimSMART are survey observations. The goal of these observations is the built-up and maintenance of a catalogue of geostationary objects. Furthermore ZIMLAT is routinely used for unresolved space object identification by means of colour photometry and light curve measurements.

This paper will highlight the space situational awareness capabilities of the Zimmerwald observatory from a technical point of view. Examples from the routine operations as well as from requests on short notice like the support of ESA during the XMM contingency operations will be given.

1 THE ZIMMERWALD OBSERVATORY

The Zimmerwald Observatory is located 10km South of Berne (Switzerland). Currently optical observations are performed with the 1m Laser and Astrometric Telescope ZIMLAT (Fig. 1) and the 0.2m Small Aperture Robotic Telescope ZimSMART (Fig. 2). Both telescopes are equipped with state-of-the-art CCD cameras with low readout-noise and high quantum efficiency (Tab. 1).

	ZIMLAT CO2	ZimSMART
Mount	azimuthal	Equatorial (Paramount)
Max. Slewing Velocity	20°/s	10°/s
RMS of positioning	< 2"	< 30"
Primary mirror	1 m	18 cm
Focal length	4000 mm	500 mm
Type	Ritchey-Cretien	Newton (Takahashi 180ED)
Camera	Astrocam 42-40	FLI09000
CCD Manufactor	E2V42-40	Kodak PL09000
CCD Area	27.6 mm x 27.6 mm	36.6 mm x 36.6 mm
Pixelcount	2048 x 2048	3056 x 3056
FOV	23' x 23'	4°06' x 4°06'
Pixel scale	0.7"/Pixel	5.0"/Pixel
Max. Quantumefficiency	95%	65%
Min. Readoutnoise	6 electrons	10 electrons
Readouttime	38 seconds	9 seconds
Limiting Magnitude (exptime 5s)	19 mag	16 mag
RMS of astrometric postions	0.1"	0.7"

Table 1: Comparison between technical data of ZIMLAT and of ZimSMART

ZIMLAT (installed in 1997) is used either for laser ranging to satellites (SLR) or for optical observation of positions and magnitudes of near-Earth objects. During daytime the system operates in SLR mode only. During nighttime the available observation time is shared between SLR and CCD using negotiated priorities. The switching between the modes is done under computer control and needs less than half a minute. In addition light curves and photometric observations can be retrieved.

Due to the large field of view (FOV) ZimSMART (installed in 2006) is best suited for sky surveys. The goals of these surveys are mainly to build-up and maintain a catalogue of artificial satellites and space debris objects.
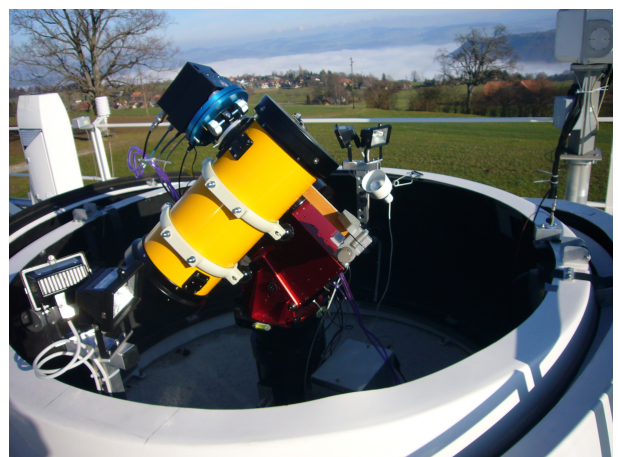

Figure 1: Image of ZIMLAT

Figure 2: Image of ZimSMART

2 ASTROMETRIC OBSERVATIONS

2.1 ZIMLAT observations 2005-2008

ZIMLAT is especially used for follow-up observations of newly detected small-size space debris objects. These objects were either discovered by the ESA space debris telescope in Tenerife [1] (campaign hprsat) or by observatories of our international partners, in particular the International Scientific Optical Network ISON [2] led by the Keldysh Institute of Applied Mathematics KIAM (campaign ESAjointsat). The resulting positions and orbital elements are shared among the partners. ZIMLAT observations play a key role in the maintenance of orbits of objects with high area-to-mass ratios. Since 2005 follow-up observations of 121 objects discovered by the ESA space debris telescope were performed. Without these observations it would be impossible to build-up a catalogue of these objects. In addition observations for scientific studies (campaigns longgeo, gto_long) and calibration (campaign GPS) were performed (Fig. 3 and 4). Looking at the magnitude distribution of all observations (Fig. 5) there is a significant decrease in the number of observations fainter than 16mag. This decrease is caused by the limiting magnitude of the optical system (about 19mag). The peak in the interval between 12 and 13mag is induced by GNSS observations for calibration purposes.
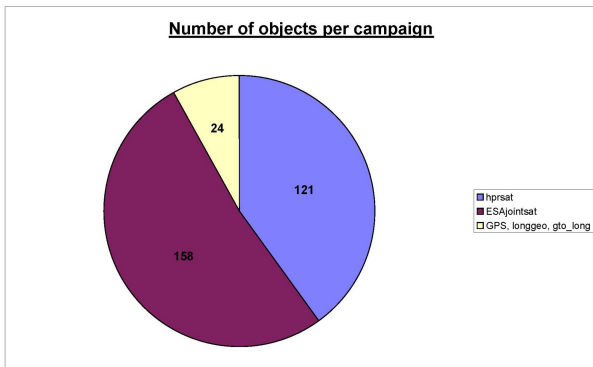

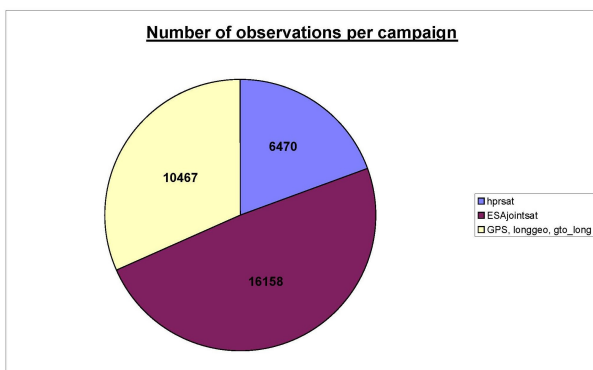Figure 3: Number of objects per campaign observed by ZIMLAT since 01-01-2005

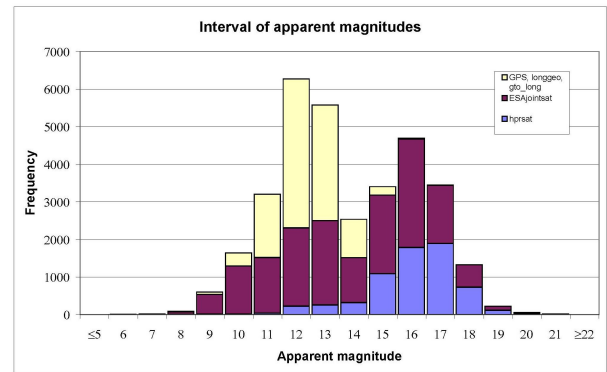Figure 4: Number of observations per campaign observed by ZIMLAT since 01-01-2005

Figure 5: Magnitude distribution of all observations with ZIMLAT since 01-01-2005

2.2 ZimSMART observations 2008

The main tasks of the ZimSMART Telescope are Sky Survey and Follow-up observations. Sky Surveys are performed by scanning of declination stripes with constant right ascension. Each stripe consists of 4 fields so each stripe has a size of 4 x 16 degrees[2]. During the acquisition the telescope is looking in a direction fixed with respect to the Earth. For each field there are 5 images taken with an exposure time of 5 seconds. The time difference between the acquisitions of each stripe is about 15 minutes. On these series an automatic object identification algorithm is looking for tracklets of objects. During the last 6 months more than 10000 tracklets have been found. This number is not identical with the number of objects due to the fact that more than one tracklet can belong to the same object. The decrease in the magnitude distribution (Fig. 6) is again caused by the limiting magnitude of the optical system (about 16mag).
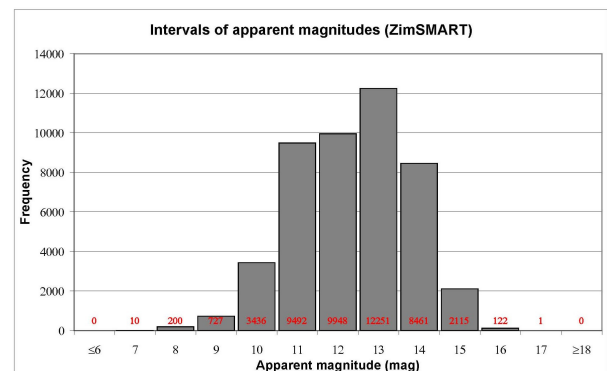

Figure 6: Magnitude distribution of all observations with ZimSMART since 01-09-2008

2.3 Accuracy of optical satellite observations

The accuracy of astrometric observations of objects depends mainly on the accuracy of the parameters of the inner and exterior orientation of the image and the accuracy of the measured positions of the objects relative to reference stars. For fast moving objects relative to the sky background the recording of the exact

starting and end time is very crucial. Errors in the exposure time induce errors in the measured position in alongtrack direction. For geostationary satellites an error of 7ms causes an alongtrack error of 0.1 arcseconds and corresponds to the RMS of the astrometric positions of ZIMLAT. For satellites in lower orbits the errors are even higher. This accuracy can hardly be achieved by taking the shutter signal as reference for your exposure time due to the following reasons: On the one hand the delay between sending a signal for opening and closing the shutter and the reaction of the shutter may vary with the ambient air temperature, on the other hand the time for opening and closing will probably not be identical. This asymmetry causes different exposure times depending on the distance from the centre of the image.

AIUB developed a special acquisition mode, the so-called smearmode, to meet the demands concerning the accuracy of the exposure times. The smearmode allows the registration of the exposure time within 1ms regardless of the shutter signals and operates in the following way:

1. The camera receives the command to expose and read the CCD.
2. While the shutter begins to open, the CCD stays in clearing mode for a user pre-programmed length of time sufficient to allow the shutter to completely open. Subsequently the clearing is stopped and a pulse is sent to mark the beginning of the pre-programmed exposure time set.
3. Just after the exposure time ends, another pulse is sent to signal the end of the exposure and the clearing begins again for a pre-programmed length of time while the shutter closes.
4. Subsequently the clearing stops and the CCD is read normally.

You can recognize the smearmode by faint trails on brighter objects (Fig. 7). This mode is implemented in the software for the Astrocam 42-40 camera.
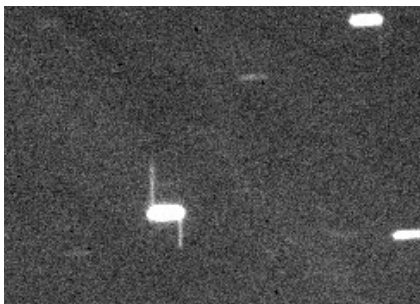

Figure 7: Characteristic faint trails on brighter objects

Due to the higher RMS of the astrometric positions (0.7 arcseconds) in comparison to observations of ZIMLAT (0.1 arcseconds) the requirements concerning the accuracy of the exposure time are much lower (by a factor of 7). An accuracy of 10ms can be achieved for the camera FLI09000, mounted on ZimSMART, with the help of calibration measurements. Positions of GNSS satellites are compared to the much more precise microwave observations to calibrate the exposure time registration. This approach has indicated a systematic offset in alongtrack direction of the ZimSMART observations caused by systematic errors in the recording of the exposure times of 0.03 seconds. This offset is caused by the delay between sending a signal for opening and closing the shutter and the reaction of the shutter. After taking this delay into consideration the maximum difference in right ascension and declination does not exceed 3 arcseconds (Fig. 8).
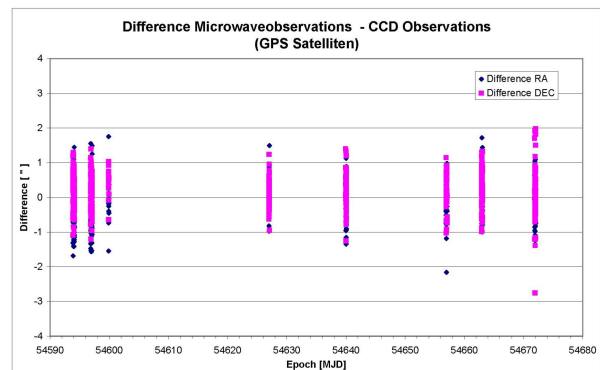

Figure 8: Difference of microwave observations with respect to CCD Observations in right ascension (RA) and declination (DEC) for GPS Satellites

2.4 LONG-TIME MODELLING OF ORBITS EXEMPLIFIED BY THE COOLER COVER OF MSG-2 (05049E)

EUMETSAT's weather satellites MSG-2 was launched from Kourou, French Guiana on December 22, 2005. Just prior to reaching operational altitude the cooler cover was ejected in a special manoeuvre, several hundred kilometres away from the geostationary orbital plane, ensuring that they cannot come into contact with other operational satellites. On January 4, 2006 AIUB could take images of the cooler cover. During the observation the telescope was looking in a direction fixed with respect to the Earth. The cooler cover appears as dot as it is nearly stationary with respect to the Earth rotation. The stars appear as lines (Fig. 9).
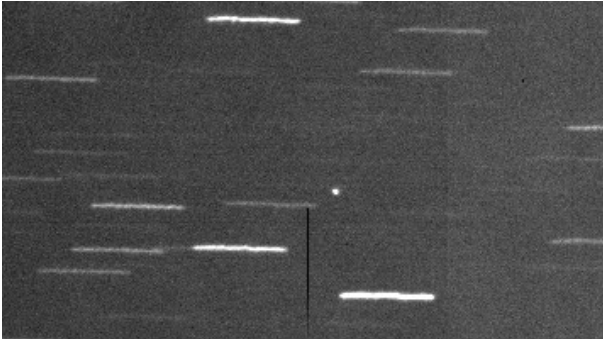
Figure 9: Image of 05049E

For the maintenance of a catalogue long-time modelling of orbits is of special interest. The better an orbit can be modelled the longer can be the time interval between follow-up observations. Beside the six osculating elements, dynamic parameters have to be considered in the orbit determination.
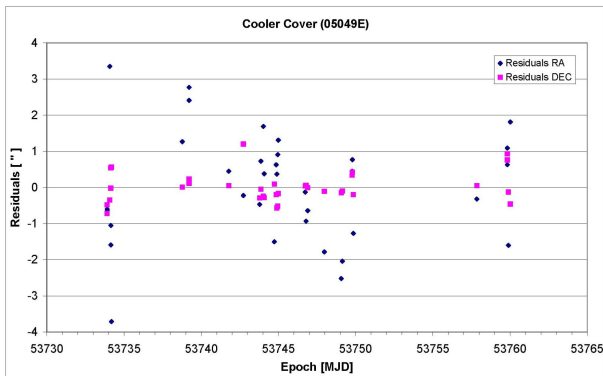

Figure 10: Residuals of observations of 05049E for the best fitting perturbed orbit (arc length 26 days)

```
ORBIT DETERMINATION FOR OBJECT 05049E00
SATELLITE  1    ARC       =        1
                FROM (MJD)  = 53733.904
                TO (MJD)    = 53760.022
                # OBS-EPOCHS =       34
                # ITERATIONS =       10
---------------------------------------
OSCULATING ELEMENTS AND THEIR RMS ERRORS
****************************************
OSCULATION EPOCH = 53733.9041948 MJD
SEMIMAJOR AXIS   =   41917476.978 M  +-       4.584 M
REV. PERIOD U    =      1423.483 MIN
ECCENTRICITY     =   0.0001448250 --- +-0.0000019167
INCLINATION      =      1.8150413 DEG +- 0.000076491
R.A. OF NODE     =   -112.4507519 DEG +- 0.002361134
ARG OF PERIGEE   =    207.1190336 DEG +- 1.326831486
ARG OF LAT AT T0 =    148.2800312 DEG +- 0.002371182
****************************************

NUMBER OF DYNAMICAL PARAMETERS  :  4
DECOMPOSITION TYPE (1=RSW, 2=DYX): 1
****************************************
PARAMETER = S0 VALUE =0.136019D-08 +-0.708270D-10 M/S**2
PARAMETER = SC VALUE =0.273310D-06 +-0.441413D-07 M/S**2
PARAMETER = SS VALUE =-.261445D-06 +-0.477025D-07 M/S**2
****************************************
PARAMETER = DRP  VALUE =0.588668D+01 +-0.489857D+00
****************************************
SAT  1 : RMS=  1.21"  # OBS =  68 # PARMS = 10 BETA= -24.12 GRAD
```

Figure 11: Orbital elements of 05049E (34 observations, arc length 26 days, output from program SATORB)

These dynamic parameters are mainly the direct solar radiation pressure and the accelerations in alongtrack direction. For uncontrolled objects the determination of these parameters is crucial. Those objects perform an attitude motion, which can hardly be modelled. Two examples are given for the long-time modelling, both modelled with the program SATORB [5] for the cooler cover of MSG-2. First model represents the orbit of one month, the second one the orbit of approximately one year.

The following a priori force field was used:
- ļ Earth potential up to degree and order 6
- ļ Gravitational attraction from Sun and Moon
- ļ Earth tides
- ļ Direct radiation pressure

The following parameters were estimated:
- ļ Six Keplerian elements
- ļ Scaling factor for direct radiation pressure (DRP)
- ļ Along track acceleration (S)
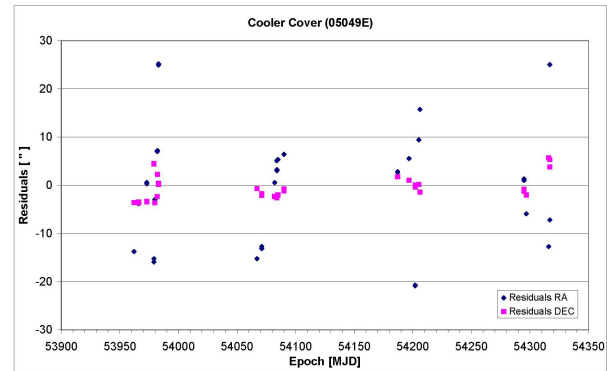- ļ Once per revolution terms in along track direction (SC, SS)

Figure 12: Residuals of observations of 05049E for the best fitting perturbed orbit (arc length 354 days)

```
ORBIT DETERMINATION FOR OBJECT 05049E00
SATELLITE  1    ARC       =        1
                FROM (MJD)  = 53962.062
                TO (MJD)    = 54316.940
                # OBS-EPOCHS =       36
                # ITERATIONS =       10
---------------------------------------
OSCULATING ELEMENTS AND THEIR RMS ERRORS
****************************************
OSCULATION EPOCH = 53962.0616781 MJD
SEMIMAJOR AXIS   =   41918112.350 M  +-       4.320 M
REV. PERIOD U    =      1423.516 MIN
ECCENTRICITY     =   0.0011876216 --- +-0.0000290516
INCLINATION      =      1.3154598 DEG +- 0.000543184
R.A. OF NODE     =   -129.3303514 DEG +- 0.025140934
ARG OF PERIGEE   =    260.9720242 DEG +- 0.850864798
ARG OF LAT AT T0 =    101.6396716 DEG +- 0.025161066
****************************************

NUMBER OF DYNAMICAL PARAMETERS  :  4
DECOMPOSITION TYPE (1=RSW, 2=DYX): 1
****************************************
PARAMETER = S0 VALUE =-.817200D-10 +-0.321969D-11 M/S**2
PARAMETER = SC VALUE =0.102431D-07 +-0.448649D-08 M/S**2
PARAMETER = SS VALUE =0.300414D-07 +-0.279966D-08 M/S**2
****************************************
PARAMETER = DRP  VALUE =0.235142D+01 +-0.428273D-01
****************************************
SAT  1 : RMS=  9.16"  # OBS =   72 # PARMS = 10 BETA=  15.48 GRAD
```

Figure 13: Orbital elements of 05049E (36 observations, arc length 354 days, output from program SATORB)

In both cases the rms error of a single observation (1.2 resp. 9.2 arcseconds) is significantly larger than the measurement noise of 0.2 arcseconds (Fig. 10 – 13) due to an insufficient radiation pressure model.   Although

the orbit model cannot represent the observations correctly, the object will be inside the field of view of ZIMLAT even when no follow-up observations can be performed within months.

3   PHOTOMETRIC OBSERVATIONS

3.1   Light curves

During the searches for debris in the geostationary transfer orbit region a new population of objects has been found in unexpected orbits where no potential progenitors exist [3]. Temporal photometry (light curves) have been acquired with the ZIMLAT telescope to study the nature of these debris [4]. The light curves have been received by taking series of small subframes centred round the object with an exposure time of a few seconds. On these subframes the intensity of the object is measured without any reduction like dark or flat field correction. Some light curves show strong variations over short time intervals (Fig. 14) where other light curves do not show strong variations (Fig. 15).
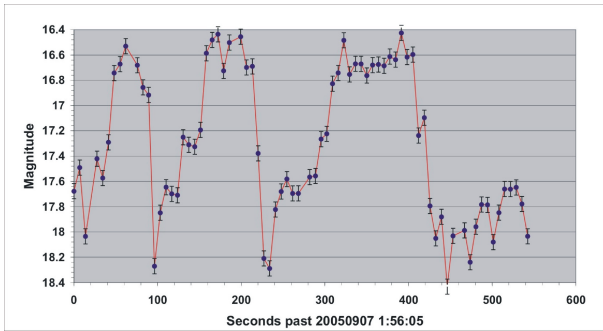

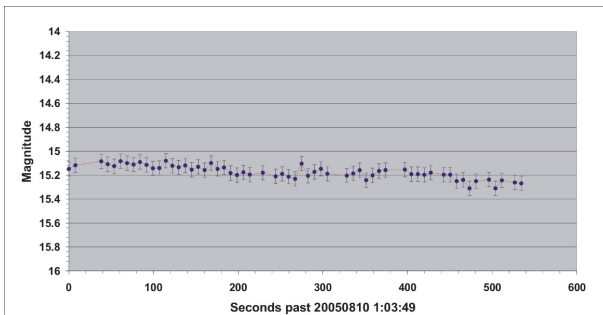*Figure 14: Light curve of the object 'EGEO21' which has an area-to-mass ratio of 4.6 m^2/kg.*

Figure 15: Light curve of the object 'EGEO14' which has an area-to-mass ratio of 17 m^2/kg.

3.2   Photometric observations

Photometric observations consist of taking full frames in the Johnson-Cousins BVRI bands and using reference stars in the field of view to calibrate the instrumental magnitudes [4]. Series of consecutive exposures in three different filters are acquired in the order of V, R, I, V and so on. The exposure times are of the order of a few seconds and the time interval between two consecutive

exposures is about 15 seconds. Afterwards the colour-indices V-I and R-I are calculated and averaged.

The scatter in the figures is dominated by the intrinsic brightness variations of the objects. The accuracy of a single photometric measurement is of the order of 0.05mag for both objects. The colour indices for solar type stars are (V-I) ~ 0.6mag and (R-I) ~ 0.35mag. The object EGEO33 (Fig. 16) thus seems to be blue while the object EGEO45 (Fig. 17) has a more white-like colour.
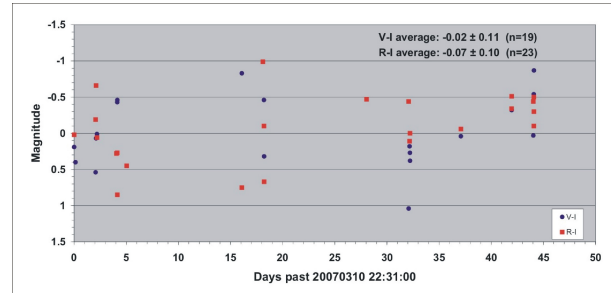

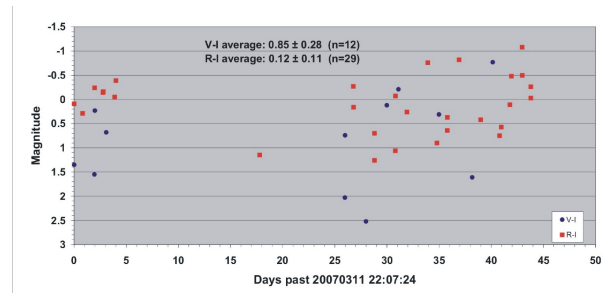*Figure 16: V–I and V–R colour indices of object EGEO33 (area-to-mass ratio = 5.4 m^2kg^{-1}).*

Figure 17: V–I and V–R colour indices of object EGEO45 (area-to-mass ratio = 17 m^2kg^{-1}).

4   THE XMM NEWTON X-RAY TELESCOPE CONTINGENCY OPERATIONS

During the weekend October 19/20, 2008 ESA lost contact to its XMM-Newton X-ray telescope. AIUB was asked for optical observations on short notice. On October 20 optical observations were first performed unsuccessfully by ZIMLAT due to an alongtrack error in the TLEs. With the aid of ZimSMART this alongtrack error could be estimated. Afterwards XMM observations were also performed with ZIMLAT (Fig. 18).
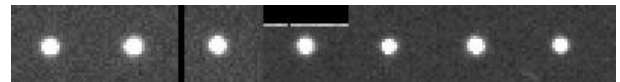

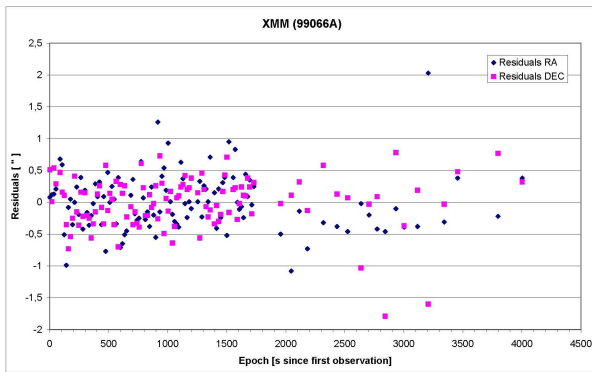*Figure 18: Image series of XMM-Newton in the night October 27/28, 2008*

Figure 19: Residuals of observations of XMM for the best fitting perturbed orbit.

An orbit was estimated using both ZIMLAT and ZimSMART observations. No systematic offset can be seen between observations of the two telescopes (Fig. 19).

In addition light curves were calculated using observations from both telescopes (Fig. 20). The magnitudes were corrected for varying range. There is clearly no signature of any attitude motion (rotation or tumbling) with a period smaller than a few hours.
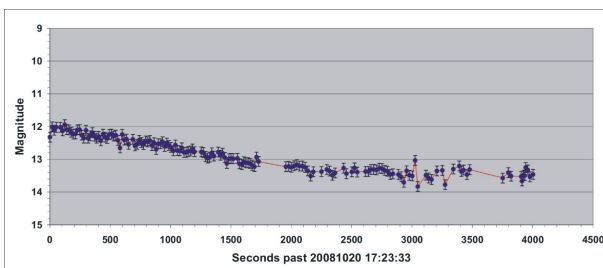

Figure 20: Light curve of XMM-Newton

5 REFERENCES

[1] T. Schildknecht, R. Musci, W. Flury, J. de Léon Cruz, and L. de Fatima Dominguez Palmero. *Optical Observations of Space Debris in High-Altitude Orbits*. In Proceedings of the Forth European Conference on Space Debris, pp. 113-118, ESOC, Darmstadt, Germany, 18-20 April 2005, 2005.

[2] V. Agapov, I. Molotov, and V. Titenko. *The ISON International Observation Network – Latest Scientific Achievements and the Future Works*. In Paper presented at the 37th COSPAR Scientific Assembly, Montreal, Canada, 13-20 July 2008, 2005.

[3] T. Schildknecht, R. Musci, T. Flohrer. *Properties of the High Area-to-Mass Ratio Space Debris Population at High Altitudes*. 36th COSPAR Scientific Assembly, July 16-23, Beijing, China, 2006, Advances in Space Research, Vol. 41, pp 1039–1045.

[4] T. Schildknecht, R. Musci, C. Früh, M. Ploner. *Color Photometry and Light Curve Observations of Space Debris in Geo*. In Proceedings of the 59th International Astronautic Conference, Glasgow 29 Sep – 3 Oct, 2008.

[5] G. Beutler. *Methods of Celestial Mechanics*. Two volumes. Springer-Verlag, Heidelberg, 2005. ISBN: 3-540-40749-9 and 3-540-40750-1.